New Journal of Physics
An Institute of Physics and Deutsche Physikalische Gesellschaft Journal

Exploring the colours of dark light

M V Berry
H H Wills Physics Laboratory, Tyndall Avenue, Bristol BS8 1TL, UK
URL: http://www.phy.bris.ac.uk/staff/berry_mv.html

New Journal of Physics **4** (2002) 74.1–74.14 (http://www.njp.org/)
Received 2 September 2002, in final form 24 September 2002
Published 21 October 2002

Abstract. A previously calculated universal pattern (Berry M V 2002 *New J. Phys.* **4** 66) describes colours near an isolated phase singularity (diffraction zero), generated with white light and visible when the dark light of the singularity is scaled to isoluminance. Here the pattern is illustrated in several different situations: near the zeros of random and regular superpositions of plane waves, and near the zeros inside and outside the diffraction pattern decorating the geometrical cusp catastrophe. The universal colours emerge in miniature, close to the zeros, when an initially achromatic diffraction pattern is perturbed by switching on an asymptotic 'chromaticity parameter', that can be chosen in several different ways.

1. Introduction

As part of the recent revival (Nye 1999, Soskin and Vasnetsov 2001, Vasnetsov and Staliunas 1999) of interest in phase singularities (Nye and Berry 1974), attention has focused on strong spectral distortions near zeros of diffraction patterns formed by polychromatic (e.g. white) light (Gbur *et al* 2002a, 2002b, Foley and Wolf 2002, Ponomarenko and Wolf 2002, Popescu and Dogariu 2002). This inspired a study (Berry 2002, hereinafter called I) of the associated colours that would be seen by a human observer near an isolated zero. 'Isolated' here means that the complex wave amplitude $\psi(\boldsymbol{R}, k)$ varies linearly with position $\boldsymbol{R}$ over the spatial range considered, and linearly with wavenumber k over the visible range.

The result of the analysis in I, where the infinite-dimensional space of spectra is projected to the three-dimensional space of colours, is the distinctive universal pattern reproduced in figure 1. The colours appear when the region near the singularity, which is dark, is scaled to have constant luminosity. There is a symmetry axis, indicating the direction in which the zero moves with k. Approximately circular regions of colour, including intense blue, red and yellow, separated by a large white circle, merge into an unsaturated 'asymptotic white'. As can be seen, and as was explained in I, the region in the total gamut of possible colours that the universal pattern occupies is rather small; most notably, there is no green.

1367-2630/02/000074+14$30.00

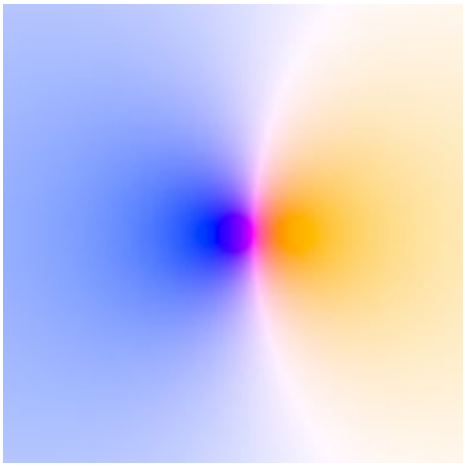

Figure 1. Universal colour pattern near an isolated phase singularity (reproduced from figure 7(h) of I).

Figure 1, and also the figures to follow, show the pattern for flat illumination, that is a source whose intensity is independent of k over the visible range. The pattern for a blackbody source with temperature $T = 4500$ K is very similar, and the main effect of varying T is to add a colour cast that alters the asymptotic white (redder for smaller T, bluer for larger). Apart from this weak dependence on the spectrum of the source, the pattern of figure 1 is universal: it represents the colours near any isolated diffraction zero, up to linear scaling and distortions.

The purpose of this paper is to show by several examples how the universal pattern of figure 1 emerges in the appropriate asymptotic limit of an isolated singularity. To generate this limit, we begin by producing achromatic diffraction patterns, that is patterns independent of k. This seems oxymoronic—a violation of the very essence of diffraction—but in fact it is not paradoxical. Several methods of generating colourless fringes are known, for example using Lloyd's mirror (Wood 1967), or the quantum mechanical achromatic 'gravity's rainbow' for falling neutrons (Berry 1982). Here a simple method using diffraction gratings is proposed. When generated with white light, the pattern is white everywhere, with an intensity falling to zero (i.e. black) at the zeros.

The achromatic fringes are then perturbed with a 'chromaticity parameter' ε so as to depend weakly on k. This introduces colours, which are strongest near the zeros, where the spectrum of the diffraction pattern is most sensitive to perturbation. However, these are also the darkest parts of the pattern, and in order to reveal the colours it is necessary to scale the pattern to constant intensity. This intensity-magnifying scaling, embodied in equation (3) of the next section, can be implemented by commercial software (e.g. Mathematica$^{\mathrm{TM}}$) applied to imported experimental or theoretical images; it can be regarded as a new type of scientific instrument (a 'chromascope'), revealing previously hidden phenomena (here colours) by analogy with other magnifiers (e.g. telescopes). After scaling, as we shall see, miniature versions of figure 1 appear in the vicinity of each zero. Two very different diffraction patterns will be employed to illustrate this asymptotic emergence of the universal colours: superpositions of plane waves (section 2), and the diffraction catastrophe decorating a cusped caustic (section 3).

Throughout this paper, light is modelled by scalar waves. It would be interesting to extend the analysis to predict the colours that would be seen near polarization singularities of vector waves.

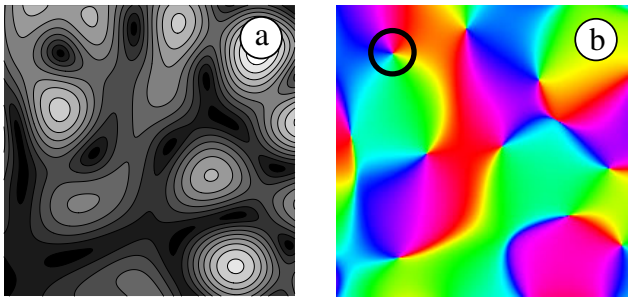

Figure 2. Achromatic superposition of $N = 20$ plane waves (equation (1)) with random phases, over the range $(-2 < (X, Y) < 2)$. (a) Contours of $|\psi|$; (b) density plot of $\arg\psi$, colour coded by hue.

2. Near-achromatic superpositions of plane waves

As the first demonstration of the universal pattern of figure 1 'in the wild', consider a sum ψ of N waves propagating in the plane, in directions $\boldsymbol{s}_n$ with phases ϕ_n, that in suitably scaled coordinates can be written

$$\psi(\boldsymbol{R}) = \sum_{n=1}^{N} \exp\{\mathrm{i}(2\pi \boldsymbol{s}_n \cdot \boldsymbol{R} + \phi_n)\}, \qquad \boldsymbol{R} = \{X, Y\},\ \boldsymbol{s}_n = \{\cos\theta_n, \sin\theta_n\}. \tag{1}$$

This is independent of k and so is achromatic, which might seem surprising. However, a method for producing wave (1) will be described at the end of this section.

Figure 2(a) is a contour map of the modulus $|\psi|$, with several zeros visible as black dots. Figure 2(b) is a density plot of the phase $\arg\psi$, with the zeros now visible as phase singularities where all colours meet; of course these hues are false colours, convenient for representing phase.

To get true colours, it is necessary to break the achromaticity of the pattern. One natural way to do this is to adopt a different spatial scaling for each wavenumber k in the mixture corresponding to the (here k-independent) white light source. A convenient scaling is

$$\boldsymbol{R} \to \left(1 + \varepsilon\left(\frac{k}{k_Y} - 1\right)\right)\boldsymbol{R}, \tag{2}$$

where ε is the chromaticity parameter, with $\varepsilon = 0$ representing achromaticity, and for convenience the scaling is centred on the wavenumber $k_Y = 2\pi/560$ nm corresponding to yellow light.

The procedure for generating and displaying the corresponding colours was fully explained in I. In outline, the spectrum at each point is first converted into three tristimulus values by integrating over the three functions $\bar{u}_i(\lambda) = \{\bar{u}(\lambda), \bar{v}(\lambda), \bar{w}(\lambda)\}$ representing the spectral responses (functions of wavelength λ) of the three cones in the eye. The $\bar{u}_i(\lambda)$ can be accurately represented by Gaussians (equation (9) of I with the source spectrum $S_0(k) = 1$); therefore the integrations can be performed analytically for the intensity $|\psi|^2$ corresponding to the wave (1) with the k-scaling (2). The tristimulus values are then converted to the three RGB values for displaying on a computer monitor, incorporating the characteristics of the monitor being used, including nonlinearity and a procedure for representing out-of-gamut colours (Hamilton 1999, 2001).

Figure 3 shows the colours for several values of ε. For small ε, where the zeros are isolated, the colours are almost entirely hidden in the darkness. As ε increases, the patterns get more strongly coloured, but then the zeros are no longer isolated and the theory of I no longer applies.

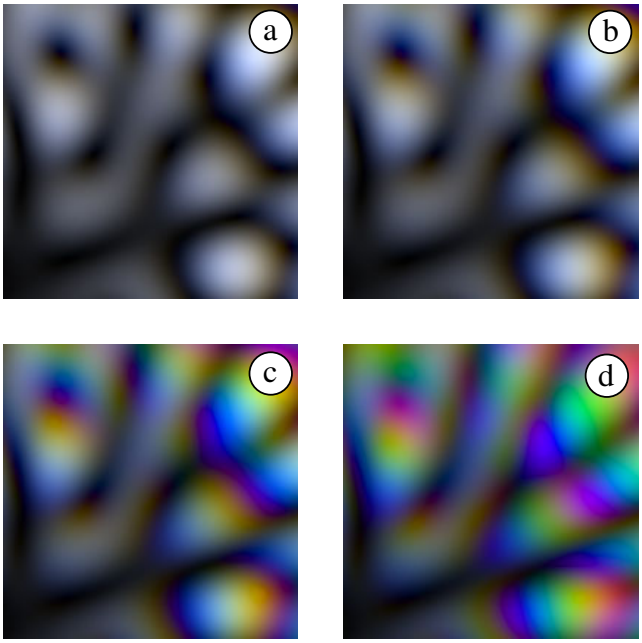

Figure 3. Simulation of the colours corresponding to figure 2, with chromaticity introduced by scaling (2), with chromaticity parameters (a) $\varepsilon = 0.1$; (b) $\varepsilon = 0.2$; (c) $\varepsilon = 0.5$; (d) $\varepsilon = 1.0$. The intensity is unscaled, so the phase singularities in figure 2 are the darkest parts of the image.

To reveal the colours, the RGB values at each point are scaled to isoluminance by the transformation

$$\begin{pmatrix} R \\ G \\ B \end{pmatrix} \Rightarrow \begin{pmatrix} R \\ G \\ B \end{pmatrix} \Big/ \max(R, G, B). \tag{3}$$

This 'chromascope' preserves the ratios between the three RGB values while making the biggest one equal to unity, so the corresponding point of the image is as bright as possible. It should be emphasized, however, that scaling (3) is a definition, appropriate for the present purpose of revealing colours in the dark parts of images. It does not produce an image where the brightness is strictly uniform, as can be seen for example by converting any of the 'isoluminated' figures to follow into greyscale images, or by noting that 'pure white' ($\{R, G, B\} = \{1, 1, 1\}$) is brighter than 'pure red' ($\{R, G, B\} = \{1, 0, 0\}$). It would be possible to produce genuinely uniform brightness, by employing a different normalization than (3) (for example dimming the whitest areas or desaturating the purer hues), but these alternatives are both unsatisfactory and unnecessary.

Figure 4 shows the dramatic result of procedure (3). For small ε, the pattern is weakly coloured almost everywhere, except in the vicinity of each achromatic zero, where a tiny representation of the universal pattern of figure 1 can be discerned. To show this more clearly, figures 5–7 are magnifications of figures 2–4 centred on one of the zeros. From figure 7 in particular it is clear how the colours for small ε are a distorted version of figure 1, with the resemblance diminishing as ε increases and the zero becomes less well isolated.

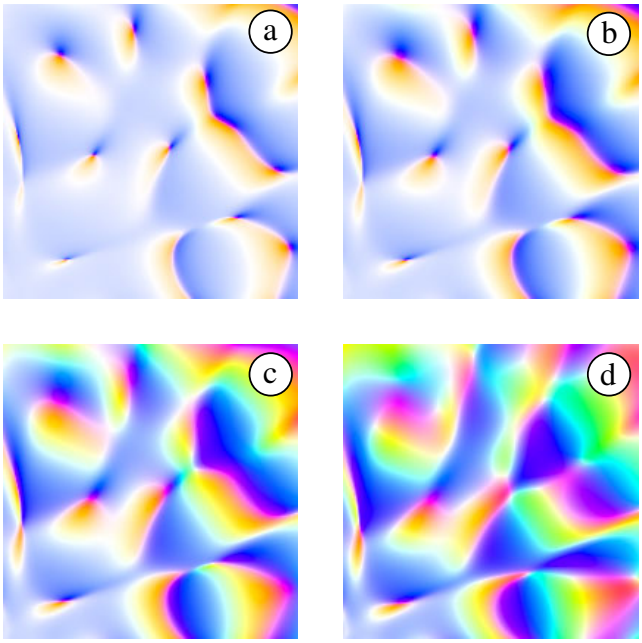

Figure 4. As figure 3, but with the intensity scaled to isoluminance according to (3).

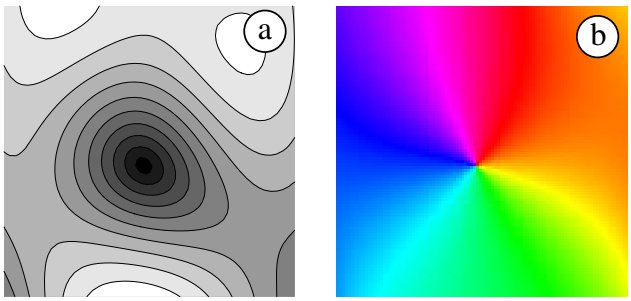

Figure 5. Magnification of figure 2 centred on the zero shown circled in figure 1(b); the range is $(0.1 < X < 0.7, 1.4 < Y < 2.0)$.

Figure 8 shows modulus and phase in a single unit cell of the periodic achromatic wave given by (1) with $N = 3$ and the directions $\theta_n = \{0, 2\pi/3, 4\pi/3\}$ and the phases $\phi_n = 0$. The pattern contains several zeros. We illustrate the robustness of the universal pattern of figure 1 by choosing a different chromaticity scaling, in which k-dependence is introduced into (1) through the phases rather than the position variables. The scaling is

$$\{\phi_n\} \to \varepsilon \frac{k}{k_Y} \{\phi_n\}, \tag{4}$$

where we choose $\phi_n = \{0, 2\pi/3, 4\pi/3\}$.

Figure 9 shows simulations of the colours for different ε, and figure 10 shows the corresponding pictures with the intensity scaled to isoluminance according to (3). Again the colours near the zeros for small ε are muddy and indistinct without the scaling, but appear strikingly in the isoluminant representation.

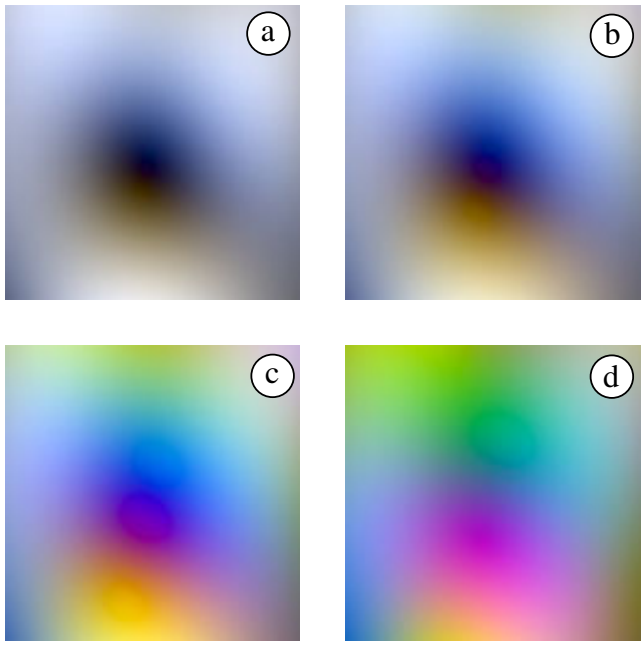

Figure 6. Magnification of the simulations in figure 3.

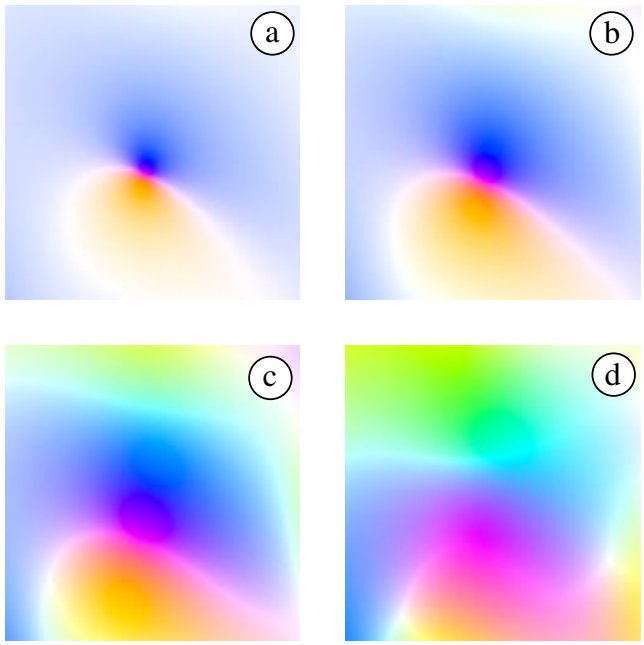

Figure 7. Magnifications of the isoluminant simulations of figure 4.

A way to generate the achromatic superposition (1) is illustrated in figure 11. N identical transparent diffraction gratings are laid flat round a circle with their rulings tangential to the circle, and illuminated from below. Each grating transmits plane waves in directions corresponding to the different orders m of diffraction, and these plane waves overlap in a region above the centre of the circle. If the gratings are small enough in comparison with the radius of the circle, the

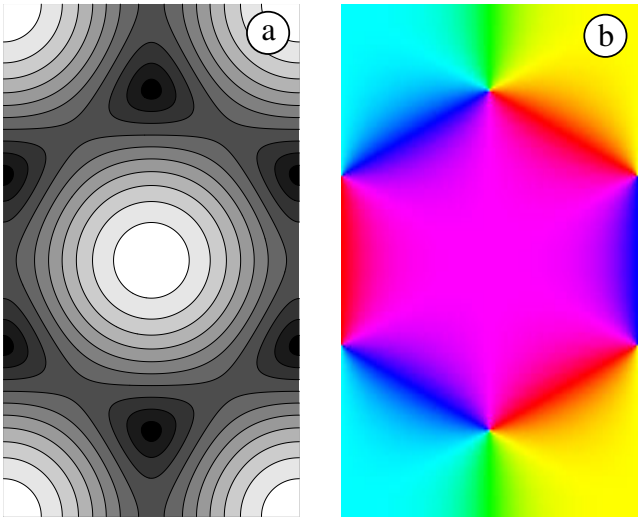

Figure 8. Achromatic superposition of $N = 3$ plane waves (equation (1)) with phases $\phi_n = 0$, in the unit cell $(0 < X < 2/3, 0 < Y < 2/\sqrt{3})$. (a) Contours of $|\psi|$; (b) density plot of $\arg\psi$, colour coded by hue.

different orders m will be spatially separated. Then the interference in $\boldsymbol{R}$ planes of constant height is between the mth-order diffracted waves from each of the N gratings. This gives, for given order m, the wave

$$\Psi_m(\boldsymbol{R}, k) = \sum_{n=1}^{N} \exp\left\{\mathrm{i}\left(\frac{2\pi m}{a}\boldsymbol{s}_n \cdot \boldsymbol{R} + z_n\left(\sqrt{k^2 - \left(\frac{2\pi m}{a}\right)^2} - k\right)\right)\right\}, \tag{5}$$

where a is the separation between lines on the gratings, $\boldsymbol{s}_n$ are the unit normals to the rulings of the gratings and z_n are the heights of the gratings, allowing for their not being precisely in the same plane.

If all the z_n are the same, the phase factor involving k is common to all the terms in the sum, so the intensity $|\boldsymbol{\Psi}_m|^2$ is independent of k and the interference pattern is achromatic, as desired. The scale of the interference fringes is determined by the grating constant a, rather than by the wavelengths in the incident light. It is slightly surprising that a diffraction grating, whose familiar application is to separate the different wavelengths in white light, that is, to introduce chromaticity, can also be employed for the opposite purpose of making achromatic fringes.

If the individual gratings are not precisely at the same height, that is if the z_n are different, the superposition contains k-dependent phases, representing chromaticity, and expansion of these phases over the visible range (e.g. about k_Y) gives a scaling of the form (4). Alternatively, if all the z_n are equal, (4) can be implemented by placing different chromatic phase-shifting slabs above each grating (e.g. different thicknesses of a dispersive material such as glass).

3. Near-achromatic cusp diffraction catastrophe

Very different manifestations of the universal colours near diffraction zeros occur in the interference patterns decorating the stable geometrical (ray) caustics described by catastrophe theory

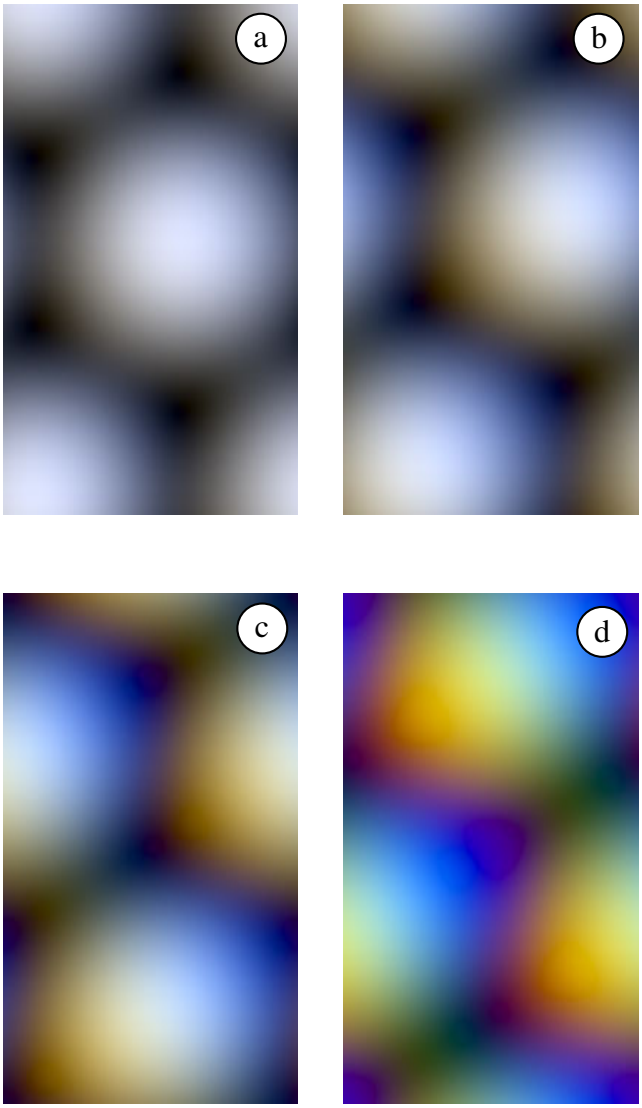

Figure 9. Simulation of the colours corresponding to figure 8, with chromaticity introduced by scaling (4), with chromaticity parameters (a) $\varepsilon = 0.2$; (b) $\varepsilon = 0.5$; (c) $\varepsilon = 1.0$; (d) $\varepsilon = 2.0$. The intensity is unscaled, so the phase singularities in figure 8 are the darkest parts of the image.

(Berry and Upstill 1980, Nye 1999). The simplest such diffraction catastrophe possessing zero points in the plane is the cusp, whose associated wave is described by the integral (Pearcey 1946)

$$P(\boldsymbol{R}) = \int_{-\infty}^{\infty} \mathrm{d}t \exp\{\mathrm{i}(\tfrac{1}{4}t^4 + \tfrac{1}{2}Yt^2 + Xt)\}. \tag{6}$$

Figure 12 shows the modulus and phase of $P(\boldsymbol{R})$; there are zeros inside the geometrical cusp, forming a distorted lattice, and the cusp is flanked by a single row of zeros on each side (Berry *et al* 1979).

To introduce chromaticity, we scale the coordinates as in (2). This choice of uniform scaling in X and Y might seem surprising, in view of the well known anisotropic k-scaling when diffraction catastrophes are generated by reflection or refraction (Berry and Upstill 1980), in

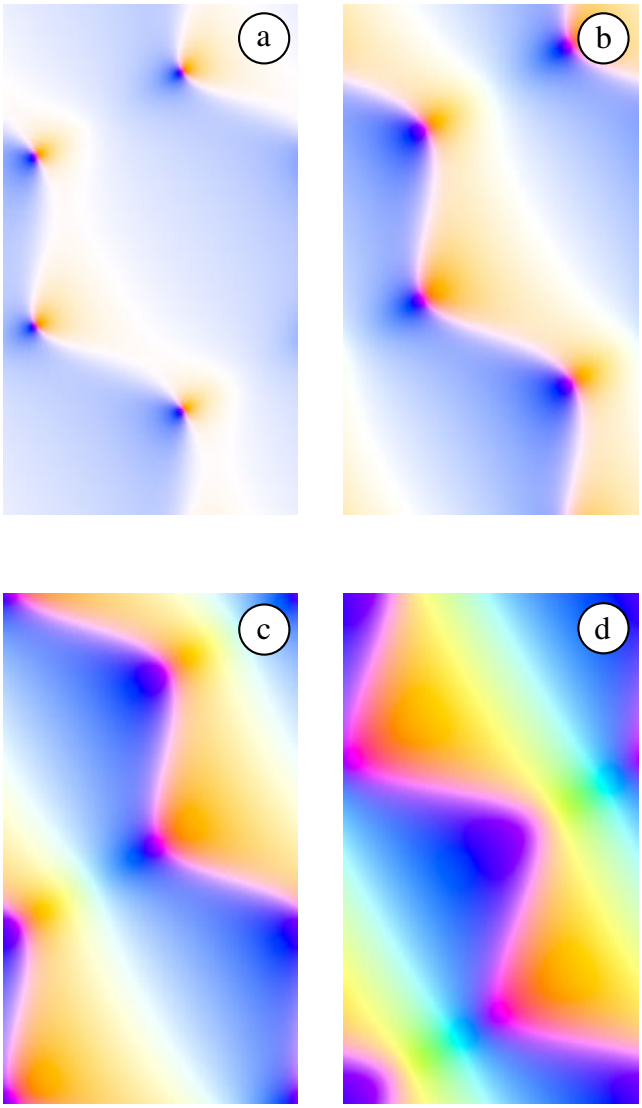

Figure 10. As figure 9, but with the intensity scaled to isoluminance according to (3).

which X scales as $1/k^{3/4}$ and Y scales as $1/k^{1/2}$. However, the uniform scaling is appropriate for the method to be proposed later for generating an achromatic cusp. Moreover, the pictures generated by the more familiar anisotropic scaling look very similar to those obtained by the local k-scaling (2).

The infinite oscillatory integral representing Pearcey's function (6) must be evaluated numerically, so there is no advantage in using the Gaussian representations of the three spectral response functions $\bar{u}_i(\lambda)$ to obtain the tristimulus values and thence the colours of the pattern. Instead, standard tabulations (Kaye and Laby 1973) of the $\bar{u}_i(\lambda)$ at 81 different values of λ must be employed to evaluate the integrals over the spectrum as sums. This was done at each point of a lattice of 57 181 points covering the range shown in figure 12.

Figure 13 shows the resulting colour simulations. For small ε, the colours are very faint. For larger ε, the colours are stronger, and resemble those studied experimentally and theoretically

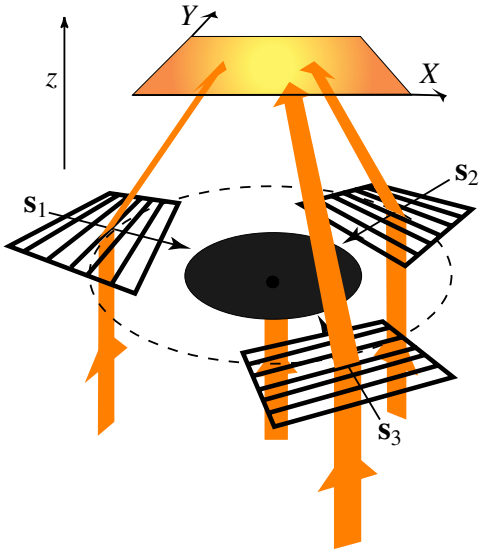

Figure 11. Gratings arranged round a circle; overlapping mth-order diffracted waves produce an achromatic interference pattern in the $\boldsymbol{R} = \{X, Y\}$ plane.

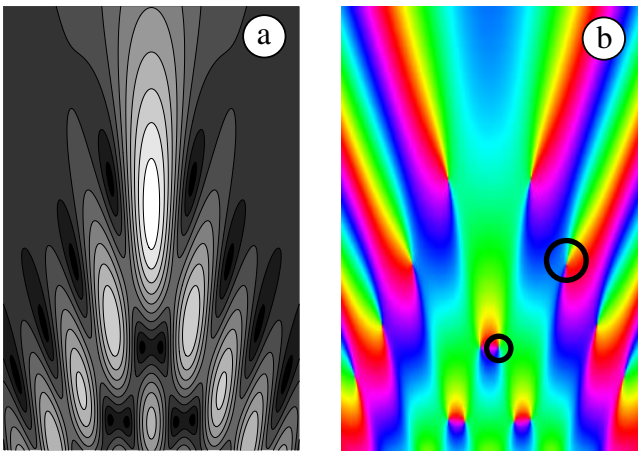

Figure 12. Achromatic cusp diffraction catastrophe (6) (Pearcey pattern) in the range $(-6 < X < +6, -6 < Y < +1)$. (a) Contours of $|P|$; (b) density plot of $\arg P$, colour coded by hue.

by Berry and Klein (1996). As figure 14 shows, the isoluminant representation again reveals the universal colours decorating the zeros for small ε.

The zeros inside and outside the cusp look different; this can be seen more clearly by magnifying one of each. Figure 15 shows a zero inside the cusp; the isoluminant representation clearly displays the pattern of figure 1. Figure 16 shows a zero outside the cusp; now the universal pattern is greatly stretched along its symmetry direction, illustrating the possibility (incorporated into the theory given in I) that the universal pattern may appear with linear distortion.

Creating an achromatic cusp seems difficult. One possible way is through the curvilinear diffraction gratings studied by Lee (1983) (see also Nye *et al* 1987), whose principle is as

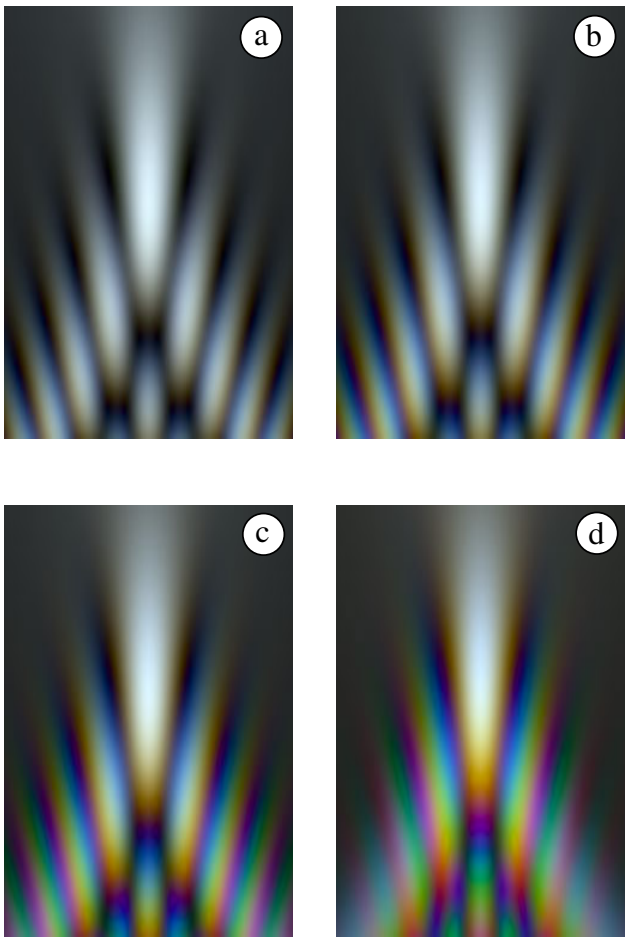

Figure 13. Simulation of the cusp diffraction colours corresponding to figure 12, with chromaticity introduced by scaling (2), with chromaticity parameters (a) $\varepsilon = 0.1$; (b) $\varepsilon = 0.2$; (c) $\varepsilon = 0.5$; (d) $\varepsilon = 1.0$. The intensity is unscaled, so the phase singularities in figure 12 are the darkest parts of the image.

follows. Instead of having lines periodic in X or Y, these gratings have a transparency function T depending periodically on a nonlinear function $h(\boldsymbol{r})$. If $T(h + a) = T(a)$, then Fourier expansion gives

$$T(h(\boldsymbol{r})) = \sum_{m=-\infty}^{\infty} T_m \exp\left\{\mathrm{i}2\pi m \frac{h(\boldsymbol{r})}{a}\right\}. \tag{7}$$

The terms labelled by m represent different orders of diffraction. Each propagates as though generated by a transparent object producing a phase shift proportional to $h(\boldsymbol{r})$, for example glass undulating according to a landscape whose contours are the lines of the grating. It is possible to arrange the geometry such that the patterns corresponding to different m are separated. Elementary diffraction theory gives the corresponding far-field pattern as

$$\boldsymbol{\Psi}_m(\boldsymbol{R}, k) = \int\int \mathrm{d}\boldsymbol{r} \exp\left\{\mathrm{i}\left(2\pi m \frac{h(\boldsymbol{r})}{a} + k\mu(k)\boldsymbol{r}\cdot\boldsymbol{R}\right)\right\}, \tag{8}$$

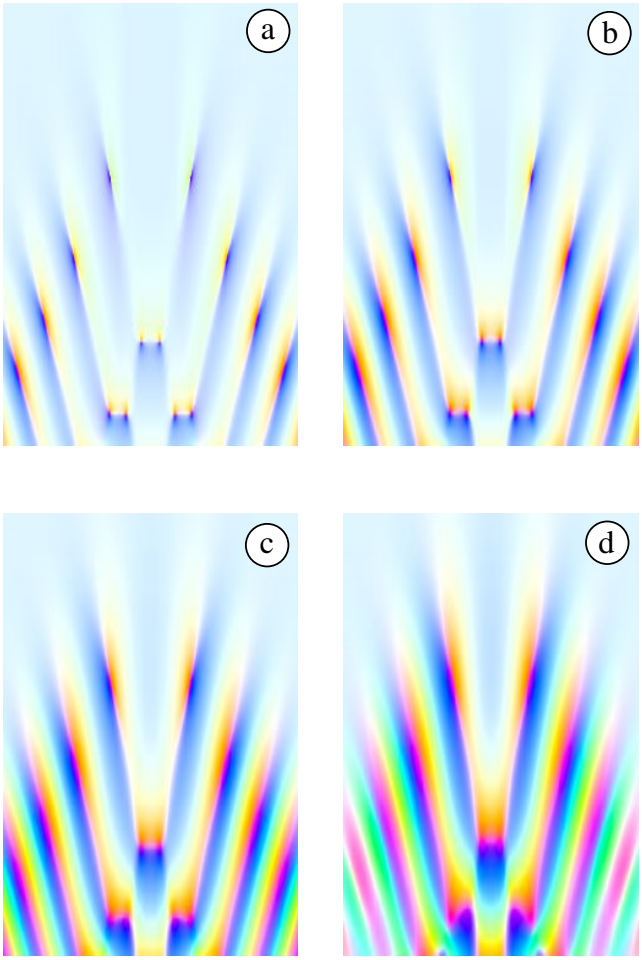

Figure 14. As figure 13, but with the intensity scaled to isoluminance according to (3).

where now $\boldsymbol{R}$ represents angular coordinates corresponding to a distant observation plane, and $\mu(k)$ is the refractive index in which the waves propagate away from the grating. Lee (1983) shows that a cusp in the far field can be generated (i.e. (8) can be transformed into (6)) by choosing

$$h(\boldsymbol{R}) = \frac{x^4}{\Delta^3} + \frac{x^2 y}{\Delta^2} + \frac{y^2}{\Delta}, \tag{9}$$

where Δ is an appropriate distance.

The wave (8) is 'half-way achromatic', in the sense that the 'grating' part of the phase, involving h, is independent of k, but the 'propagation' part, depending on $\boldsymbol{R}$, does depend on k. Complete achromaticity could however be achieved by choosing $\mu(k) \sim 1/k$, representing a medium with strong negative dispersion. A slight failure to achieve this, for example

$$\mu(k) = \mu_Y \left(\frac{k_Y}{k}\right)^{1-\varepsilon}, \tag{10}$$

corresponds to the chromaticity scaling (2) after expansion in $k - k_Y$. This is admittedly contrived but demonstrates that the envisaged conditions could be realized, at least in principle.

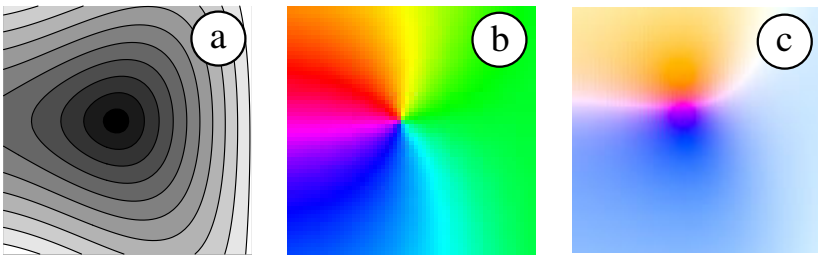

Figure 15. Magnification of zero within the cusp near $X = 0.45$, $Y = -4.38$ (shown circled in figure 12(b)), in the range $(0.1 < X < 0.7, -4.7 < Y < -4.1)$: (a) achromatic, contours of $|P|$; (b) achromatic, contours of $\arg P$; (c) isoluminant colours, $\varepsilon = 0.1$.

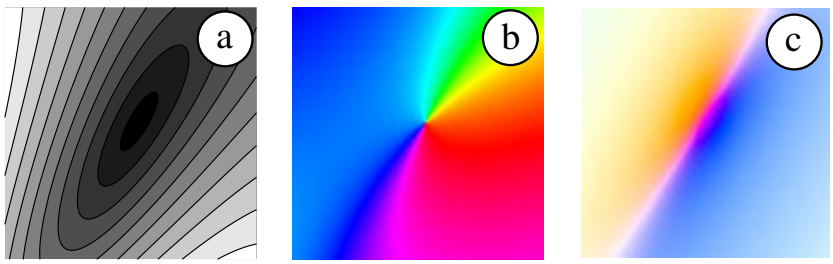

Figure 16. Magnification of zero outside the cusp near $X = 3.1$, $Y = -3.08$ (shown circled in figure 12(b)), in the range $(2.6 < X < 3.6, -3.6 < Y < -2.6)$: (a) achromatic, contours of $|P|$; (b) achromatic, contours of $\arg P$; (c) isoluminant colours, $\varepsilon = 0.1$.

4. Concluding remarks

The universal colour pattern of figure 1 has been shown to emerge asymptotically in the limit where zeros are isolated, that is the achromatic limit $\varepsilon \to 0$. Thus the colour pattern of phase singularities joins a list of asymptotically emergent universal phenomena in physics. Other examples are critical phenomena (where universal scaling exponents emerge close to critical points in the thermodynamic limit), diffraction catastrophes (where characteristic patterns decorating caustics emerge in the short-wave limit) and random-matrix spectra in quantum systems that are classically chaotic (where universal level correlations emerge in the semiclassical limit of highly excited states).

An asymptotic parameter that can be tuned to best display the phenomenon under study is convenient for theoretical purposes and for demonstration experiments like the diffraction arrangement of figure 11, proposed in section 2. However, in natural optical fields the asymptotic parameter may be an unavailable luxury. Then, the zeros in a diffraction field should be examined individually; they can be more or less isolated, and the theory of I will apply to a greater or lesser degree, depending on circumstances. An example is the naturally coloured cusp generated experimentally by Berry and Klein (1996, figure 3(b)). When transformed to isoluminance according to (3), the most isolated zero, namely one of the two flanking the caustic and closest to the cusp point, just begins to show aspects of the universal structure of figure 1. Evidently, more experiments are needed.

Acknowledgment

I thank Professor J F Nye for several comments and helpful suggestions.

References

Berry M V 1982 Wavelength-independent fringe spacing in rainbows from falling neutrons *J. Phys. A: Math. Gen.* **15** L385–8

—— 2002 Coloured phase singularities *New J. Phys.* **4** 66 (denoted I in the text)

Berry M V and Klein S 1996 Colored diffraction catastrophes *Proc. Natl Acad. Sci. USA* **93** 2614–19

Berry M V, Nye J F and Wright F J 1979 The elliptic umbilic diffraction catastrophe *Phil. Trans. R. Soc.* A **291** 453–84

Berry M V and Upstill C 1980 Catastrophe optics: morphologies of caustics and their diffraction patterns *Prog. Opt.* **18** 257–346

Foley J T and Wolf E 2002 The phenomenon of spectral switches as a new effect in singular optics with polychromatic light *J. Opt. Soc. Am.* A submitted

Gbur G, Visser T D and Wolf E 2002a Anomalous behavior of spectra near phase singularities of focused waves *Phys. Rev. Lett.* **88** 013901

—— 2002b Singular behavior of the spectrum in the neighborhood of focus *J. Opt. Soc. Am.* A submitted

Hamilton A J S H 1999 *Where's Purple? Or, How to Plot Colours Properly on a Computer Screen* webpage http://casa.colorado.edu/∼ajsh/colour/rainbow.html#eq3

—— 2001 *What Colour is the Sun?* webpage http://casa.colorado.edu/∼ajsh/colour/Tspectrum.html

Kaye G W C and Laby T H 1973 *Tables of Physical and Chemical Constants* (London: Longman)

Lee R A 1983 Generalized curvilinear diffraction gratings: V. Diffraction catastrophes *Opt. Acta* **30** 449–64

Nye J F 1999 *Natural Focusing and Fine Structure of Light: Caustics and Wave Dislocations* (Bristol: Institute of Physics Publishing)

Nye J F and Berry M V 1974 Dislocations in wave trains *Proc. R. Soc.* A **336** 165–90

Nye J F, Haws D R and Smith R A 1987 Use of diffraction gratings with curved lines to study the optical catastrophes D_6^+ and D_6^- *J. Mod. Opt.* **34** 407–27

Pearcey T 1946 The structure of an electromagnetic field in the neighbourhood of a cusp of a caustic *Phil. Mag.* **37** 311–17

Ponomarenko S A and Wolf E 2002 Spectral anomalies in a Fraunhofer diffraction pattern *Opt. Lett.* submitted

Popescu G and Dogariu A 2002 Spectral anomalies at wavefront dislocations *Phys. Rev. Lett.* **88** 183902

Soskin M S and Vasnetsov M V 2001 Singular optics *Prog. Opt.* **42** 219–76

Vasnetsov M and Staliunas K (eds) 1999 *Optical Vortices* (New York: Nova)

Wood R W 1967 *Physical Optics* (New York: Dover)